Electronic Supplementary Information

Addressing Vibronic Phosphorescence and Associated Excited State Dynamics of Anti-Kasha Molecules : A Time-Dependent Correlation Function Approach†

Keniya Basu,[a] Pijush Karak,[a,b] and Swapan Chakrabarti*[a]

[a] Department of Chemistry, University of Calcutta, 92, A.P.C. Road, Kolkata-700 009, India

[b] Department of Chemistry, KTH Royal Institute of Technology, SE-10044 Stockholm, Sweden.

*e-mail: swcchem@caluniv.ac.in

Contents

1 Theoretical Background

The theory for simulation of vibronically resolved phosphorescence spectra along with the calculation of nonradiative rate constants are given below.

1.1 Theory for simulation of vibronically resolved phosphorescence spectra

The explicit expression of the time-dependent correlation function corresponding to vibronic phosphorescence is

$$\chi_{\text{phos}}(t,t') = \sqrt{\frac{\det(\mathbf{S}_i)\det(\mathbf{S}_f)}{\det(\mathbf{W})}} exp(-\frac{i}{2\hbar}\mathbf{V}^{\mathrm{T}}\mathbf{W}^{-1}\mathbf{V} + \frac{i}{\hbar}\mathbf{D}^{\mathrm{T}}\mathbf{U}\mathbf{D}). \tag{1}$$

The expressions of $\mathbf{S}_f$, $\mathbf{B}_f$, $\mathbf{S}_i$, $\mathbf{B}_i$, $\mathbf{W}$, $\mathbf{U}$ and $\mathbf{V}$ in TDCF can explicitly be written as,

$$\mathbf{S}_f = \frac{\omega_f}{\sin(\omega_f t\hbar)} \tag{2}$$

$$\mathbf{B}_f = \frac{\omega_f}{\tan(\omega_f t\hbar)} \tag{3}$$

$$\mathbf{S}_i = \frac{\omega_i}{\sin(\omega_i t'\hbar)} \tag{4}$$

$$\mathbf{B}_i = \frac{\omega_i}{\tan(\omega_i t'\hbar)} \tag{5}$$

$$\mathbf{W} = \begin{bmatrix} \mathbf{B}_f + \mathbf{J}^{\mathrm{T}}\mathbf{B}_i\mathbf{J} & -(\mathbf{S}_f + \mathbf{J}^{\mathrm{T}}\mathbf{S}_i\mathbf{J}) \\ -(\mathbf{S}_f + \mathbf{J}^{\mathrm{T}}\mathbf{S}_i\mathbf{J}) & \mathbf{B}_f + \mathbf{J}^{\mathrm{T}}\mathbf{B}_i\mathbf{J} \end{bmatrix} \tag{6}$$

$$\mathbf{U} = \mathbf{B}_i - \mathbf{S}_i \tag{7}$$

$$\mathbf{V} = \begin{bmatrix} \mathbf{J}^{\mathrm{T}}\mathbf{U}\mathbf{D} \\ \mathbf{J}^{\mathrm{T}}\mathbf{U}\mathbf{D} \end{bmatrix} \tag{8}$$

respectively. In the above expressions, $\omega, \mathbf{D}$ and $\mathbf{J}$ are the normal mode frequencies, displacement vectors and Duschinsky rotation matrix, respectively. The relation between the Duschinsky rotation matrix and normal coordinates of the initial ($\mathbf{Q}_i$) and final ($\mathbf{Q}_f$) electronic states is given by $\mathbf{Q}_f = \mathbf{J}\mathbf{Q}_i + \mathbf{D}$. $\mathbf{S}$ and $\mathbf{B}$ are diagonal matrices whereas $\mathbf{W}$ and $\mathbf{U}$ are $(2N \times 2N)$ and $(N \times N)$ matrices, respectively and $\mathbf{V}$ is a $(2N \times 1)$ column vector. Once the correlation function is evaluated in the time domain, fast Fourier transform in the West (FFTW) has been utilized to convert the data in the frequency domain.

1.2 Theory for the calculation of ISC rate constants

1.2.1 Direct spin-orbit coupling induced Intersystem crossing

The Fermi's Golden rule based expressions of $k_{\text{ISC}}^{\text{DSO}}$ between S_i and T_f can be written as

$$\mathrm{k}_{\mathrm{ISC}}^{\mathrm{DSO}} = \frac{2\pi}{\hbar z}\sum_{\substack{v_{\mathrm{S_i}} \\ v_{\mathrm{T_f}}}} e^{-\beta E_{v_{\mathrm{S_i}}}} \left|\left\langle \mathrm{S_i}, v_{\mathrm{S_i}} \middle| \hat{H}_{\mathrm{SO}} \middle| \mathrm{T_f}, v_{\mathrm{T_f}} \right\rangle\right|^2 \times \delta(\Delta E_{\mathrm{ST}} + E_{v_{\mathrm{S_i}}} - E_{v_{\mathrm{T_f}}})$$

In terms of time-dependent correlation function, the final expressions of $\mathrm{k}_{\mathrm{ISC}}^{\mathrm{DSO}}$ can be given as,

$$k_{\mathrm{ISC}}^{\mathrm{DSO}} = \frac{|\mathrm{H_{SO}}|^2}{\hbar^2 z}\int_{-\infty}^{\infty} G_{\mathrm{DSO}}^{\mathrm{ISC}}(t,t') e^{i\Delta E_{\mathrm{ST}}\frac{t}{\hbar}} dt \tag{9}$$

The expression of the matrix element of $\mathrm{H_{SO}}$ is

$$\mathrm{H_{SO}} = \langle \mathrm{S_i}|\hat{H}_{\mathrm{SO}}|\mathrm{T_f}\rangle. \tag{10}$$

$G_{\mathrm{DSO}}^{\mathrm{ISC}}(t,t')$ in Eqs. 9 is the time-dependent correlation function expression for the DSO-assisted ISC mechanisms. The form of t' is $-\frac{t}{\hbar} - i\beta$ where t is the real time.

The general expression of correlation function ($G_{\mathrm{DSO}}^{\mathrm{ISC}}(t,t')$)for ISC can be given as,

$$G_{\mathrm{DSO}}^{\mathrm{ISC}}(t,t') = \sqrt{\frac{\det(\mathbf{S}_i)\det(\mathbf{S}_f)}{\det(\mathbf{W})}} exp(-\frac{i}{2\hbar}\mathbf{V}^{\mathrm{T}}\mathbf{W}^{-1}\mathbf{V} + \frac{i}{\hbar}\mathbf{D}^{\mathrm{T}}\mathbf{U}\mathbf{D}). \tag{11}$$

So the final form of the equation becomes,

$$\begin{aligned}\mathrm{k}_{\mathrm{ISC}}^{\mathrm{DSO}} = \frac{|\mathrm{H_{SO}}|^2}{\hbar^2 z}\int_{-\infty}^{\infty}\sqrt{\frac{\det(\mathbf{S}_i)\det(\mathbf{S}_f)}{\det(\mathbf{W})}} \\ \times exp\Big(-\frac{i}{2\hbar}\mathbf{V}^{\mathrm{T}}\mathbf{W}^{-1}\mathbf{V} + \frac{i}{\hbar}\mathbf{D}^{\mathrm{T}}\mathbf{U}\mathbf{D}\Big) e^{i\Delta E_{\mathrm{ST}}\frac{t}{\hbar}} dt.\end{aligned} \tag{12}$$

The detailed discussion and derivation related to Eqn.11 can be found in Refs. 1–4.

1.2.2 Herzberg-Teller (HT) coupling induced Intersystem crossing

The matrix element of the perturbing Hamiltonian after the inclusion of the HT term arising from SOC is expressed as:

$$\langle S_{\mathrm{i}}, \nu_{S_{\mathrm{i}}}|\hat{H}'|T_{\mathrm{f}}, \nu_{T_{\mathrm{f}}}\rangle = \langle S_{\mathrm{i}}, \nu_{S_{\mathrm{i}}}|\hat{H}_{\mathrm{SO}}|T_{\mathrm{f}}, \nu_{T_{\mathrm{f}}}\rangle + \frac{\partial\langle S_i, \nu_{S_i}|\hat{H}_{\mathrm{SO}}|T_f, \nu_{T_f}\rangle}{\partial\mathbf{Q}}\mathbf{Q}$$

Here, the first denotes the SOC matrix element computed on the optimized equilibrium geometry and the second one is HT term, evaluated following the rule of vector differentiation. $\mathbf{Q}$ symbolizes the normal coordinate of the initial state at equilibrium geometry. Starting from Fermi's Golden rule, the rate constant of ISC including HT part will be,

$$\mathrm{k}_{\mathrm{ISC}}^{\mathrm{HT}} = \frac{1}{\hbar^2 z}\int_{-\infty}^{\infty}\sum_{m,m'} R_{m,m'}\chi_{\mathrm{HT}}^{\mathrm{ISC}}(t,t';m,m') e^{i\Delta E_{\mathrm{ST}}t/\hbar}\, dt, \tag{13}$$

where the form of $R_{m,m'}$ and $\chi_{\mathrm{HT}}^{\mathrm{ISC}}(t,t';m,m')$ are

$$R_{m,m'} = \left(\frac{\partial\langle S|\hat{H}_{\rm SO}|T\rangle}{\partial\mathbf{Q}_m}\right)\left(\frac{\partial\langle S|\hat{H}_{\rm SO}|T\rangle}{\partial\mathbf{Q}_{m'}}\right) \tag{14}$$

and

$$\chi_{\rm HT}^{\rm ISC}(t,t';m,m') = \sqrt{\frac{\det(\mathbf{S}_i)\det(\mathbf{S}_f)}{\det(\mathbf{W})}}\exp\left(-\frac{i}{2\hbar}\mathbf{V}^{\rm T}\mathbf{W}^{-1}\mathbf{V}+\frac{i}{\hbar}\mathbf{D}^{\rm T}\mathbf{U}\mathbf{D}\right) \times\left[(i\mathbf{W}^{-1})_{m,m'}+(\mathbf{W}^{-1}\mathbf{V})_m(\mathbf{W}^{-1}\mathbf{V})_{m'}\right]. \tag{15}$$

1.3 Theory for calculating Internal Conversion rate constants

The expression of IC rate constant using the FGR is written as,

$$\mathrm{k_{IC}} = \frac{1}{\hbar^2 z}\sum_{m,m'}T_{m,m'}\int_{-\infty}^{\infty}G_{\rm IC}^{\rm FC+HT}(t,t';m,m')e^{\frac{i}{\hbar}\Delta Et}dt. \tag{16}$$

Here ΔE denotes the energy gap between two electronic states of same multiplicity. $G_{\rm IC}^{\rm FC+HT}(t,t';m,m')$ is the time-dependent generating function where both the Franck-Condon and HT terms are included. $T_{m,m'}$ contains the product of two nonadiabatic coupling matrix elements and the expression of this term is

$$T_{m,m'} = -\hbar^2\langle\psi_i|\frac{\partial}{\partial\mathbf{Q}_m}|\psi_f\rangle\langle\psi_f|\frac{\partial}{\partial\mathbf{Q}_{m'}}|\psi_i\rangle. \tag{17}$$

The form of the time-dependent correlation function is

$$G_{\rm IC}^{\rm FC+HT}(t,t';m,m') = \sqrt{\frac{\det(\mathbf{S}_i)\det(\mathbf{S}_f)}{\det(\mathbf{W})}}exp(-\frac{i}{2\hbar}\mathbf{V}^{\rm T}\mathbf{W}^{-1}\mathbf{V}+\frac{i}{\hbar}\mathbf{D}^{\rm T}\mathbf{U}\mathbf{D})\times\{i\hbar\mathrm{Tr}(\mathbf{X}\mathbf{W}^{-1}) + (\mathbf{W}^{-1}\mathbf{V})^{\rm T}\mathbf{X}(\mathbf{W}^{-1}\mathbf{V})-\mathbf{Y}^{\rm T}\mathbf{W}^{-1}\mathbf{V}\} \tag{18}$$

The details of these calculations can be found in the Refs. 5–7

2 dibenzo[b,d]thiophen-2-yl (4-chlorophenyl)-methanone (ClBDBT)

The details regarding the molecule ClBDBT are given below.

2.1 NEVPT2 results performed on ClBDBT molecule

Here we present the NEVPT2 results for calculating the phosphorescence wavelength of the ClBDBT molecule. We obtained the $T_1 \rightarrow S_0$ phosphorescence wavelength at 485 nm using a (6e,8o) CAS space with the 6-311G(d,p) basis set, considering 6 triplet and 7 singlet roots. Unfortunately, we could not obtain any $T_2 \rightarrow S_0$ phosphorescence wavelength that matches with the experimental value (460 nm). Here, we present a table summarizing several NEVPT2 results obtained for the T_2 state.

Table S1: Computational Details and Excitation Wavelengths corresponding to NEVPT2 calculations performed on T_2 geometry

CAS Space	Basis Set	No. of Roots (T,S)	Wavelength (nm)
(4,4)	6-311G(d,p)	3,4	292.2
(6,5)	6-311G(d,p)	4,5	298.9
(6,6)	6-311G(d,p)	4,5	316.9
(8,8)	6-311G(d,p)	2,3	352.2
(8,8)	6-311G(d,p)	4,5	365.8
(8,8)	6-311G(d,p)	5,4	377.4
(8,8)	6-311G(d,p)	6,3	366.3
(8,8)	aug-cc-pVDZ	4,5	388.1
(8,8)	aug-cc-pVTZ	4,5	390.3
(8,8)	aug-cc-pVQZ	4,5	389.3
(8,8)	aug-cc-pVTZ	5,4	376.6
(8,8)	aug-cc-pVTZ	5,6	379.1
(8,8)	aug-cc-pVTZ	6,5	377
(8,8)	aug-cc-pVTZ	7,8	365.9
(8,8)	aug-cc-pVTZ	8,7	364.5
(8,8)	aug-cc-pVTZ	4,5	364.5
(8,8)	6-31G(d)	5,4	380.6
(8,8)	6-311G(3df,3pd)	5,4	377.8
(8,8)	6-311G++(d,p)	5,4	374
(8,8)	6-311G++(d,p)	6,3	369.2
(8,8)	6-311G++(d,p)	6,4	371.1
(8,8)	6-311G++(d,p)	6,5	383.1
(8,8)	6-311G++(d,p)	6,4	364.1
(10,9)	aug-cc-pVTZ	4,5	401.6

2.2 CASPT2 results performed on ClBDBT molecule

The results of CASPT2 calculations performed on optimized T_2 geometry are as follows.

Table S2: Computational Details and Excitation Wavelengths corresponding to CASPT2 calculations performed on T_2 geometry

CAS Space	Basis Set	No. of Roots (T)	Wavelength (nm)
(4,4)	cc-pVDZ	3	324
(8,8)	cc-pVDZ	2	340
(8,8)	cc-pVDZ	3	375
(8,8)	cc-pVDZ	5	351

2.3 NTO Results performed on different Geometries

The orbital characters obtained by performing NTO from different optimized geometries are shown here. NTO calculations are performed on respective geometries using ωB97X-D3 and 6-311++G(d,p) level of theory. Fig. S1 presents the results obtained from respective geometries.

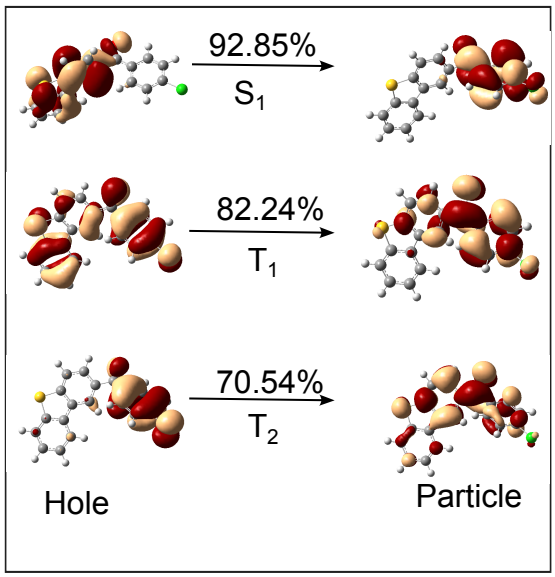

Fig. S1: NTO results obtained from respective optimized geometry

2.4 Duschinsky rotation matrix and Displacement vectors

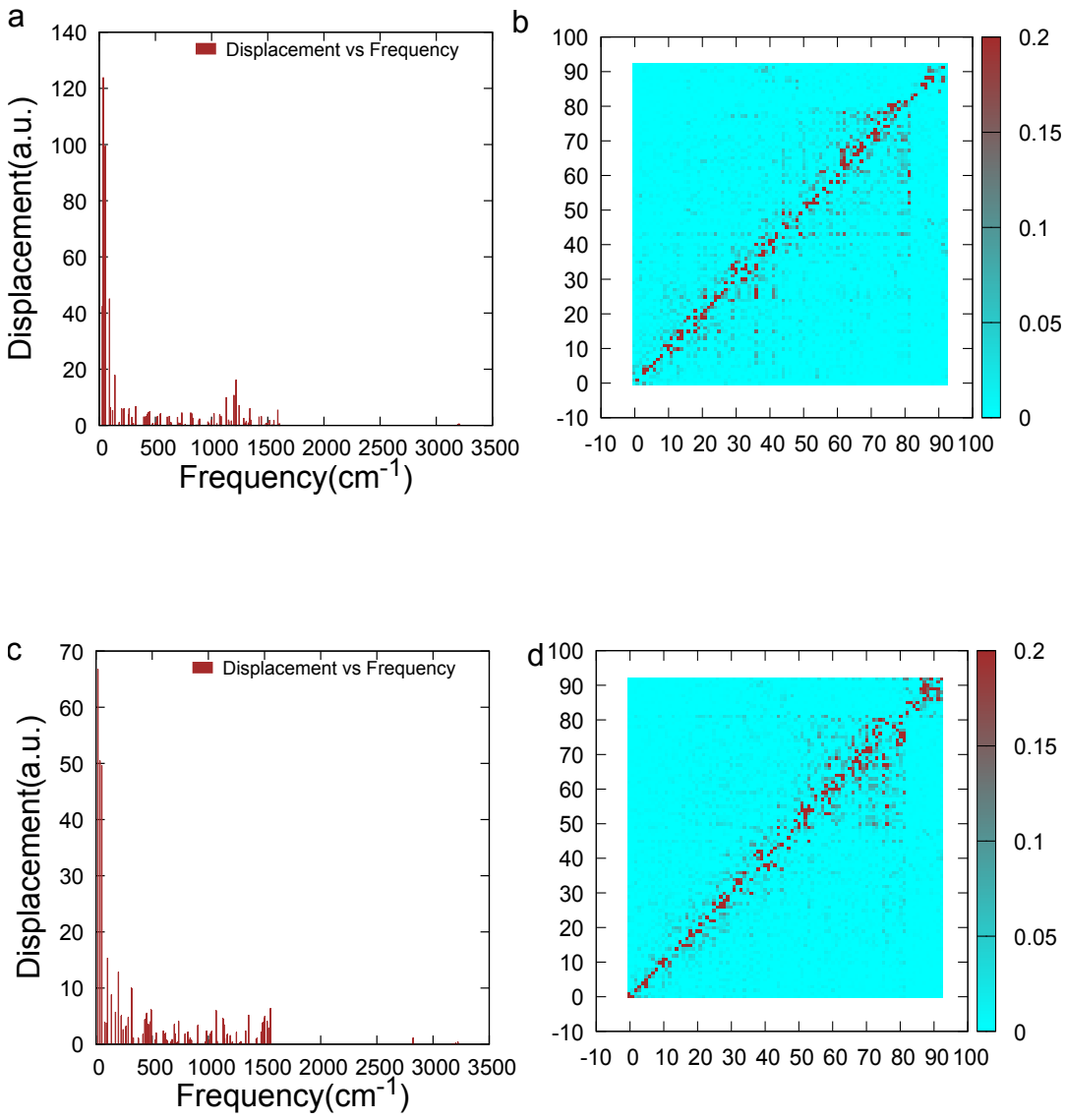

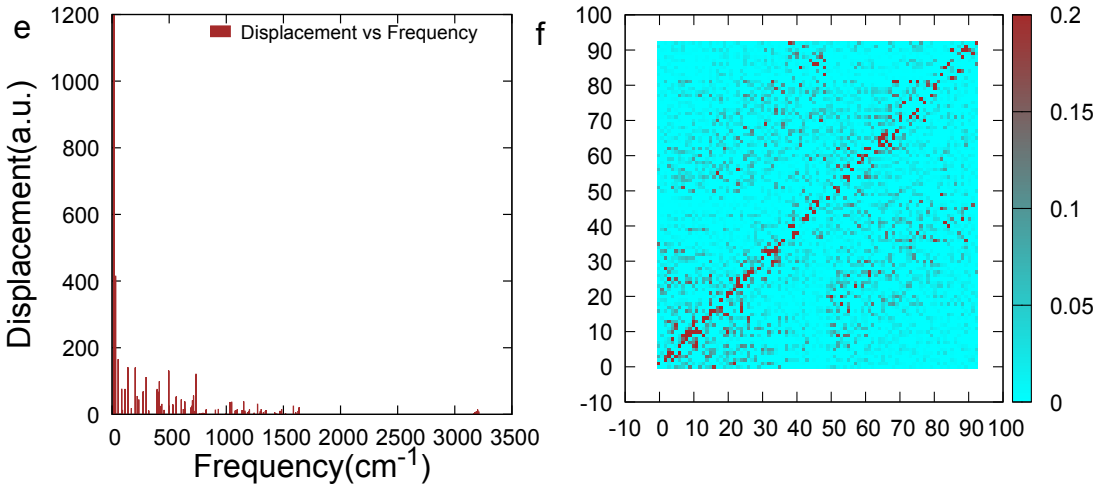
e
Displacement vs Frequency
Displacement(a.u.)
Frequency(cm-1)
f

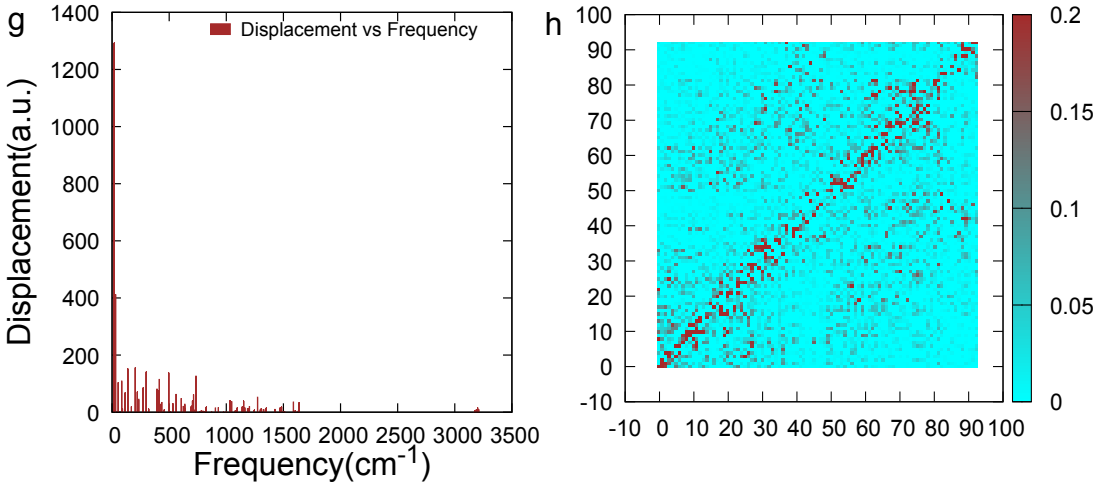
g
Displacement vs Frequency
Displacement(a.u.)
Frequency(cm-1)
h

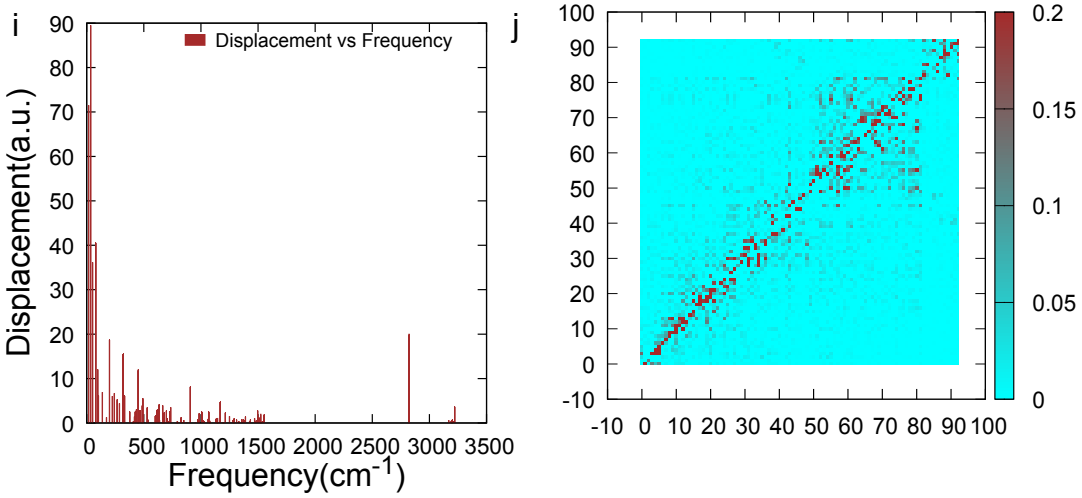
i
Displacement vs Frequency
Displacement(a.u.)
Frequency(cm-1)
j

Fig. S2: a) Plot of the displacement vector for the $T_1 \rightarrow S_0$ transition versus the vibrational frequencies of the T_1 state; (b) Plot of the Duschinsky rotation matrix obtained in cartesian coordinates between the T_1 and S_0 states. (c) Plot of the displacement vector for the $T_2 \rightarrow S_0$ transition versus the vibrational frequencies of the T_2 state; (d) Plot of the Duschinsky rotation matrix obtained in cartesian coordinates between the T_2 and S_0 states.
(e) Plot of displacement vector for the $S_1 \rightsquigarrow T_1$ transition versus the vibrational frequencies of the S_1 state; (f) Plot of the Duschinsky rotation matrix obtained in cartesian coordinates between the S_1 and T_1 states (g) Plot of displacement vector for the $S_1 \rightsquigarrow T_2$ transition versus the vibrational frequencies of the S_1 state; (h) Plot of the Duschinsky rotation matrix obtained in cartesian coordinates between the S_1 and T_2 states. (i) Plot of the displacement vector for the $T_2 \rightsquigarrow T_1$ transition versus the vibrational frequencies of the T_2 state; (j) Plot of the Duschinsky rotation matrix obtained between the T_2 and T_1 states. Here all the calculations of Duschinsky rotation matrices and displacement vectors are performed using cartesian coordinate in Fcclasses3[8] software. To maintain consistency with the previous work of Paul *et.al*[9] cartesian coordinate has been used.

2.5 NACME vs Frequency Plot

This section represents the variation of non-adiabatic coupling matrix elements between T_2-T_1 with respect to frequency values of T_2 state . Here it is observed that the mode specific NACME value corresponding to mode number 53 of T_2 state has highest value among other modes. This mode has a frequency value of 1028 cm^{-1}. So, it can be concluded that this mode contributes majorly in fast IC process between T_2-T_1 states.

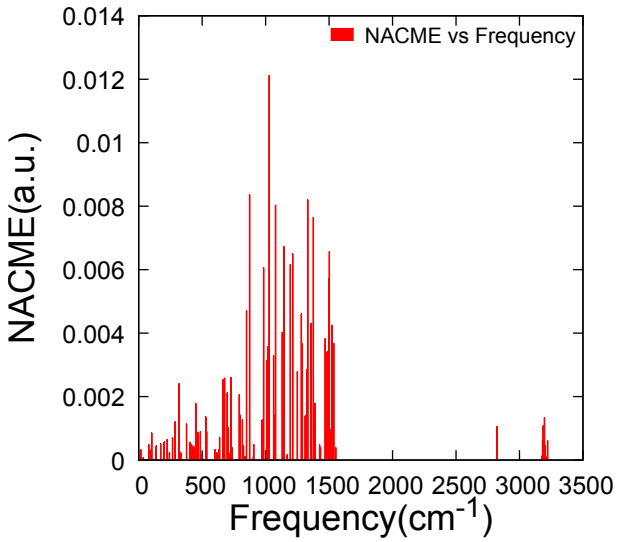

Fig. S3: Plot for NACME vs Frequency of T_2 state

2.6 Effect of Damping parameter and Temperature on Spectra

This section represents the variation of simulated phosphorescence spectra with different damping parameters and temperatures. It has been observed that with increasing temperature and damping

parameter the intensity of the peaks have decreased for both $T_1 \rightarrow S_0$ and $T_2 \rightarrow S_0$ phosphorescence of ClBDBT molecule. All the simulations here for spectral variations are performed using 10^5 number of points and a time scale of -10 ps to 10 ps.

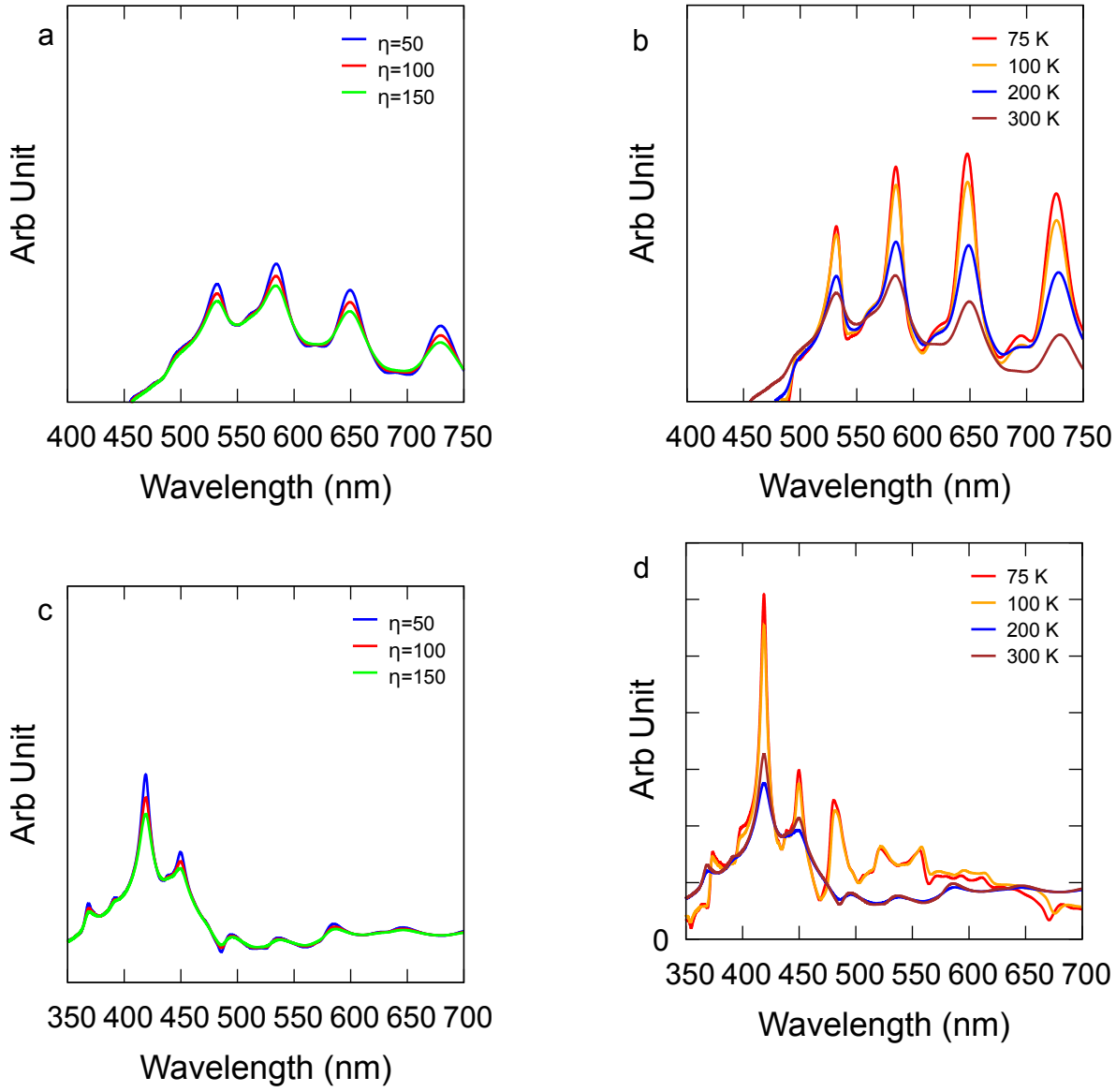

Fig. S4: Variation in the spectral features of the $T_1 \rightarrow S_0$ and $T_2 \rightarrow S_0$ phosphorescence with changes in the damping parameter (η) and temperature for the ClBDBT molecule. (a) $T_1 \rightarrow S_0$ spectral variation, with changes in the damping parameter (in cm^{-1}) at 300 K temperature. (b) $T_1 \rightarrow S_0$ spectral variation, with changes in temperature. (c) $T_2 \rightarrow S_0$ spectral variation, with changes in the damping parameter (in cm^{-1}) at 300 K temperature. (d) $T_2 \rightarrow S_0$ spectral variation, with changes in temperature.

2.7 Optimized geometry coordinate and Frequencies

The coordinates of optimized geometries of S_0, S_1, T_1, T_2 states are given below.

2.7.1 S_0 Geometry(Å)

S	-4.37448800	-0.96605500	-0.48981300
O	1.85138100	-3.16760400	0.71041000
C	-4.01466300	0.71334400	-0.06956100
C	-3.11958100	3.24227900	0.62298800
H	-2.78164100	4.23569000	0.89344100
C	-2.20848700	2.19785500	0.55812600
H	-1.16087700	2.37205500	0.77632800
C	-2.64702000	0.91428600	0.20960100
C	-1.87840000	-0.31029300	0.07838200
C	-0.50733900	-0.50698700	0.26275100
H	0.11613400	0.32519800	0.56445100
C	0.04863700	-1.77502100	0.09243900
C	-0.78255300	-2.86118800	-0.24891600
H	-0.33082400	-3.84059000	-0.34276000
C	-2.13955500	-2.68678600	-0.45428500
H	-2.76780700	-3.52541400	-0.72945500
C	-2.68276700	-1.40932900	-0.29121700
C	1.49544200	-2.05912400	0.34716800
C	2.51757800	-0.97572200	0.15753300
C	2.39611400	0.02482400	-0.81393300
H	1.52100200	0.06005600	-1.45056900
C	3.40641400	0.96395600	-0.99771300
C	4.68801700	-0.08699700	0.77587100
H	5.58156400	-0.11769400	1.38556700
C	3.68208600	-1.02990100	0.93346200
H	3.78462900	-1.82738800	1.65887000
C	-4.93448600	1.75929700	-0.00662500
C	-4.47543000	3.02369600	0.34199700
H	-5.98259600	1.59133000	-0.22364800
H	-5.17594700	3.84885600	0.39672200
C	4.53826600	0.90500600	-0.19141500
H	3.32151100	1.72952400	-1.75776700
Cl	5.80952800	2.09923100	-0.40337500

2.7.2 Frequencies

The normal mode frequencies obtained from the optimized structure of S_0 state are given below.

24.1425	35.3561	49.8161

82.8896	102.3227	117.2024
135.8839	183.3521	199.4782
239.6362	265.0039	284.1547
292.3235	326.7814	335.4166
414.0718	421.0356	430.0346
439.0757	460.6667	467.3895
482.8982	502.1933	514.0671
547.7707	575.8491	624.9650
639.5394	647.9187	695.7433
715.1382	720.5620	725.7441
729.9689	749.4464	764.9741
775.4640	831.2897	843.2690
846.2205	863.7379	866.8710
926.3833	948.0650	953.9044
982.6168	986.3725	989.2543
994.1245	1033.3048	1038.6577
1048.1874	1080.9412	1095.1657
1101.0565	1143.0112	1155.0934
1162.1146	1182.5562	1195.4944
1213.5004	1250.4106	1276.4903
1298.6665	1320.6117	1332.5139
1336.4514	1346.5866	1351.1926
1430.6697	1443.6480	1466.8615
1498.4596	1501.5751	1518.7852
1580.6588	1602.6454	1604.0098
1629.6793	1630.6928	1639.5224
1721.3891	3165.0407	3173.0720
3180.4009	3183.8776	3185.7533
3189.9656	3191.2850	3193.6962
3201.7448	3203.5576	3205.5160

2.7.3 S_1 Geometry(Å)

The optimized coordinate of S_1 state is as follows:

S	-4.00585900	-1.33205000	-1.18264600
O	1.27620700	-1.52025200	2.32057100
C	-4.31545100	0.25000600	-0.44489700
C	-4.46231300	2.69922900	0.82083900
H	-4.52955600	3.66155000	1.31350200
C	-3.27682400	1.97355900	0.88843700
H	-2.42414800	2.36727400	1.42868300
C	-3.19193900	0.73314600	0.25265100
C	-2.07090500	-0.19388300	0.19273500

C	-0.81178400	-0.08405200	0.75635800
H	-0.53946300	0.77712400	1.35294900
C	0.15200000	-1.08754600	0.52880300
C	-0.20515000	-2.26594100	-0.17759900
H	0.53553300	-3.04670100	-0.28895100
C	-1.45168500	-2.39670500	-0.74543800
H	-1.71214300	-3.27707200	-1.32006300
C	-2.38446800	-1.35832300	-0.56343200
C	1.49450100	-0.98566400	1.17587900
C	2.65820500	-0.44483300	0.63155500
C	2.69429700	0.11315400	-0.68799600
H	1.79649000	0.11689300	-1.29517600
C	3.85506000	0.64607400	-1.20211500
C	5.02998900	0.10760700	0.86500000
H	5.94511400	0.11658800	1.44414000
C	3.87593600	-0.42783800	1.39103600
H	3.87302100	-0.84508200	2.38990700
C	-5.50526000	0.96643100	-0.51887500
C	-5.56719800	2.20091200	0.12359300
H	-6.36061400	0.57789200	-1.05787000
H	-6.48279400	2.77825400	0.08061700
C	5.02657500	0.64642800	-0.42964300
H	3.87318200	1.06533300	-2.20031000
Cl	6.50870300	1.33130500	-1.09594200

2.7.4 Frequencies

16.8674	30.8989	53.5607
84.6160	91.6218	113.7247
139.0247	169.0940	202.8235
220.3901	233.7630	269.6590
271.3141	298.4824	321.5310
393.4112	406.7621	414.1323
420.6719	430.9456	434.7077
456.2057	496.6175	512.6997
532.6250	561.3449	605.8318
623.9695	637.1439	639.0808
690.6979	700.6969	703.5991
713.0517	719.0230	734.8658
765.0817	779.1450	795.7292
810.7839	822.2035	872.9704
905.0288	930.9078	940.7716
957.1077	957.2593	977.5863
996.1674	1000.7010	1032.6636
1046.7355	1074.9635	1077.8052

1094.8360	1138.6558	1152.3746
1162.3551	1185.5663	1196.2190
1202.3064	1243.8842	1273.5871
1293.7766	1297.0565	1305.3167
1324.7262	1341.4699	1347.3908
1425.4703	1440.6912	1470.8137
1476.4278	1484.4143	1497.9542
1512.6696	1519.1866	1587.7506
1601.7417	1608.1635	1629.4334
1636.3423	3167.3153	3174.9882
3181.1126	3182.7255	3187.0001
3191.6370	3192.3513	3198.8316
3199.2835	3200.7939	3209.4718

2.7.5 T_1 Geometry(Å)

The coordinate of the optimized T_1 geometry optimized by TDDFT method is as follows.

S	-4.39926000	-1.02244600	-0.46393900
O	1.81847900	-3.11888700	0.68758100
C	-4.07761400	0.67404900	-0.06966400
C	-3.24327000	3.23496200	0.57770500
H	-2.92800800	4.24063600	0.82926500
C	-2.30553300	2.21201500	0.51951300
H	-1.26051100	2.41632900	0.72289000
C	-2.71393300	0.91348800	0.19545500
C	-1.91145000	-0.29348900	0.07802400
C	-0.54839800	-0.44958700	0.28141400
H	0.05055200	0.39131200	0.60636200
C	0.06520300	-1.71136700	0.08458800
C	-0.76435900	-2.83306900	-0.23709100
H	-0.29703000	-3.80020700	-0.36219600
C	-2.12263300	-2.69005800	-0.41913700
H	-2.73124700	-3.54655600	-0.68369900
C	-2.70095000	-1.42115800	-0.27345900
C	1.47955900	-1.90807100	0.28012600
C	2.53074000	-0.94007300	0.13208900
C	2.41007700	0.18048100	-0.73180200
H	1.50647700	0.31516600	-1.31273800
C	3.44160300	1.08971100	-0.86838100
C	4.80589300	-0.22282200	0.65544500
H	5.73963300	-0.36426900	1.18453600
C	3.77098100	-1.12886700	0.80088200
H	3.88997200	-1.98424500	1.45245500

C	-5.02329800	1.69483300	-0.01366200
C	-4.59398500	2.97745000	0.31280900
H	-6.06859700	1.49675700	-0.21831600
H	-5.31561400	3.78456700	0.36131500
C	4.63795500	0.89036300	-0.17010900
H	3.33960700	1.94289700	-1.52684400
Cl	5.94679800	2.04735900	-0.34936000

2.7.6 Frequencies

28.2390	35.6999	53.4818
91.3840	99.4519	118.4216
138.4142	177.7811	199.4539
219.9899	261.3604	266.1184
290.5509	303.4989	325.5134
396.8527	411.9536	421.5743
426.7652	434.9883	447.8268
474.9551	497.0936	509.1959
518.1272	544.2182	605.7305
624.1096	635.2941	638.8473
696.8411	703.4958	711.1701
717.6389	720.9188	734.8268
763.4730	814.6904	817.7225
822.3015	832.5214	866.0351
887.0175	893.1326	949.3205
967.5575	968.7471	977.3153
990.0690	1000.5313	1020.6625
1046.8100	1072.1934	1078.1716
1084.6375	1131.2565	1151.1299
1153.1268	1176.5726	1194.5823
1198.2603	1216.8860	1245.5128
1285.7299	1297.6477	1307.4589
1326.1561	1337.2974	1341.3305
1351.3722	1422.8298	1442.2509
1469.8411	1483.0809	1492.0699
1496.6473	1516.9964	1539.4887
1554.8608	1589.0088	1603.4024
1631.1715	3166.5861	3174.5152
3179.8025	3182.6903	3185.0472
3191.0508	3191.8972	3194.5479
3200.5679	3207.8550	3210.9757

2.7.7 T_2 Geometry(Å)

The optimized coordinate of T_2 state optimized by TDDFT method taking optimized geometry of S_0 state is given below:

S	-4.42623500	-0.98254400	-0.42546400
O	1.88516600	-3.17090300	0.56762600
C	-4.05205400	0.71131700	-0.05671700
C	-3.09295500	3.26565800	0.55530800
H	-2.74405800	4.26430500	0.79124500
C	-2.18874600	2.21970500	0.49692000
H	-1.13525900	2.38870100	0.68407800
C	-2.65190000	0.90133900	0.18639700
C	-1.91020800	-0.29500700	0.07367300
C	-0.50954400	-0.48927600	0.24388600
H	0.10969300	0.34875600	0.53339700
C	0.04208400	-1.75919300	0.08954500
C	-0.79819200	-2.86096500	-0.21568000
H	-0.35239500	-3.84225500	-0.30764900
C	-2.18353000	-2.69215000	-0.39233900
H	-2.80685700	-3.54536400	-0.63068600
C	-2.72693700	-1.42861400	-0.25399300
C	1.48442300	-2.01959100	0.29106700
C	2.51295700	-0.97091800	0.13454700
C	2.39391000	0.08950600	-0.78846800
H	1.50986400	0.17056500	-1.40717100
C	3.41037300	1.02001100	-0.93429100
C	4.73153700	-0.16420600	0.72983900
H	5.64148400	-0.24803400	1.30971900
C	3.71541600	-1.09486800	0.86643600
H	3.82434600	-1.92565400	1.55124800
C	-4.94858900	1.75668300	0.00201900
C	-4.46141500	3.05280200	0.31322400
H	-6.00422100	1.60074800	-0.18389600
H	-5.15563100	3.88256500	0.36342100
C	4.57234600	0.89397100	-0.16686200
H	3.31731900	1.83358500	-1.64196400
Cl	5.85295800	2.07898700	-0.34367100

2.7.8 Frequencies

16.8916	34.5471	51.8462
79.6958	96.8597	102.6584
137.8805	173.6040	199.8841
224.5419	242.1490	266.5927

286.3812	317.5313	332.1751
376.7532	404.8594	417.8774
424.2502	434.6206	450.1960
466.3175	485.8112	491.7586
529.0162	535.5184	599.8757
615.2318	631.9564	637.5806
665.5320	677.0126	697.6419
703.5508	719.4183	727.0156
735.0415	792.5522	797.2152
817.0119	825.9667	838.4842
849.7126	873.8576	902.3665
906.8569	947.6976	972.3448
981.9902	984.6212	1008.3823
1017.7969	1028.0274	1063.1234
1069.1542	1078.1567	1131.0611
1140.0930	1145.4975	1167.9042
1194.8352	1213.1154	1250.3840
1281.3923	1289.3935	1311.7713
1325.7068	1331.6396	1358.0247
1375.8758	1389.3879	1425.6076
1433.0911	1469.4526	1483.4439
1496.5358	1501.7390	1506.9644
1523.7170	1536.7036	1552.2493
2821.9358	3169.2162	3178.8987
3181.9776	3187.1286	3190.2265
3193.5667	3196.9830	3200.9820
3205.5298	3208.0893	3221.2306

3 dibenzo[a,c]phenazine(DPPZ)

3.1 NEVPT2 results for different geometries

The results of NEVPT2 calculations performed on different optimized geometries of DPPZ molecule are as follows. 5 different orbitals shown here represents the active space orbital for above NEVPT2 calculation.

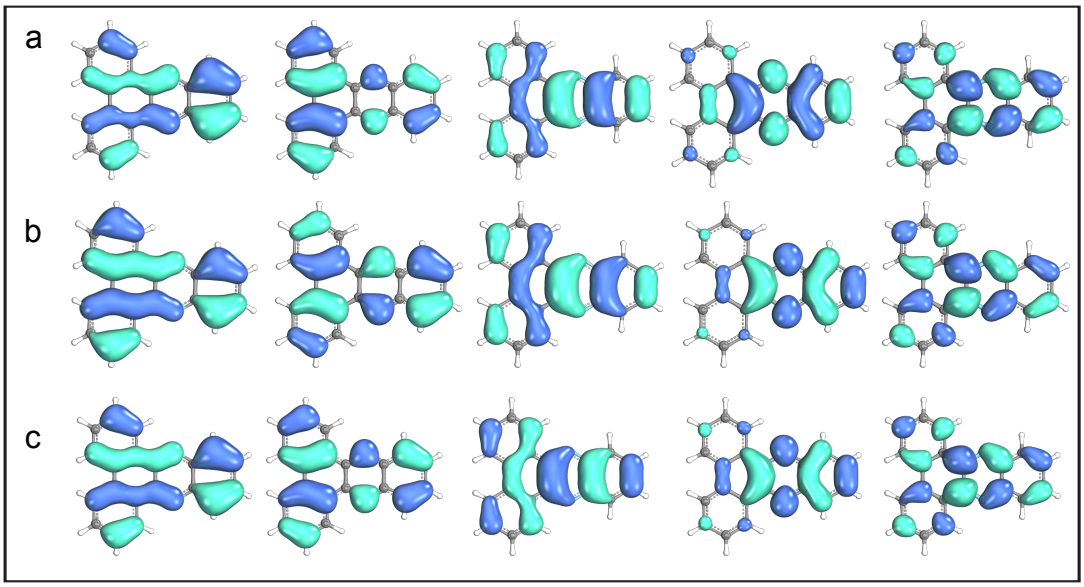

Fig. S5: NEVPT2 active orbitals obtained from S_0, T_1 and T_2 geometry. **a)** Active space orbitals obtained after a (6e,5o) NEVPT2 calculation on S_0 geometry. **b)** Active space orbitals obtained after a (6e,5o) NEVPT2 calculation on T_1 geometry. **c)** Active space orbitals obtained after a (6e,5o) NEVPT2 calculation on T_2 geometry.

3.2 NTO results performed on different geometry

The natural transition orbitals obtained from differnt optimized geometry of DPPZ molecule are shown here. Fig. S6, S7 and S8 represents the NTO results obtained from S_0, T_1 and T_2 geometries respectively. The orbital characters of S_1, T_1 and T_2 states are $\pi \rightarrow \pi^\star$ type.

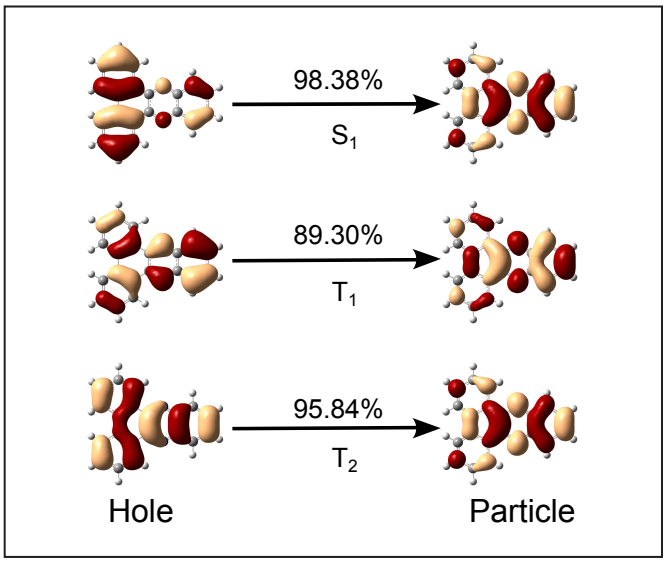

Fig. S6: NTO orbitals obtained from optimized S_0 geometry

The orbital characters obtained after performing NTO on T_1 optimized geometry are following.

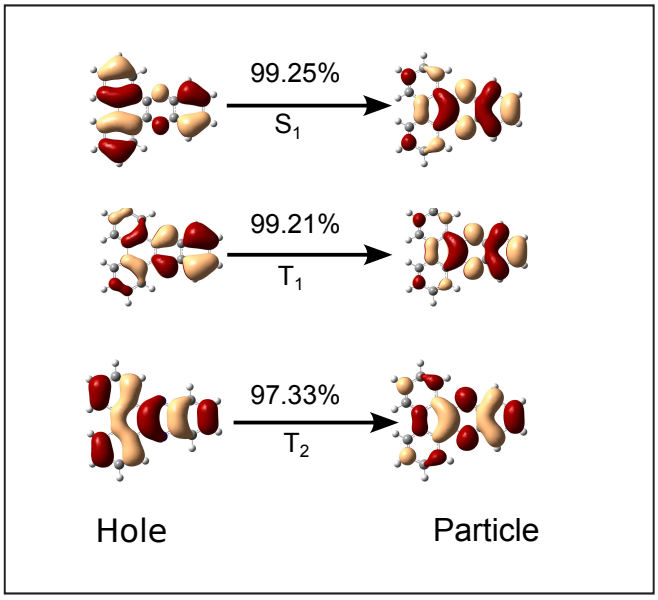

Fig. S7: NTO orbitals obtained from optimized T_1 geometry

The nature of T_1 state is of $\pi \rightarrow \pi^*$ type
Now, the orbital characters obtained after performing NTO on T_2 optimized geometry are shown below .

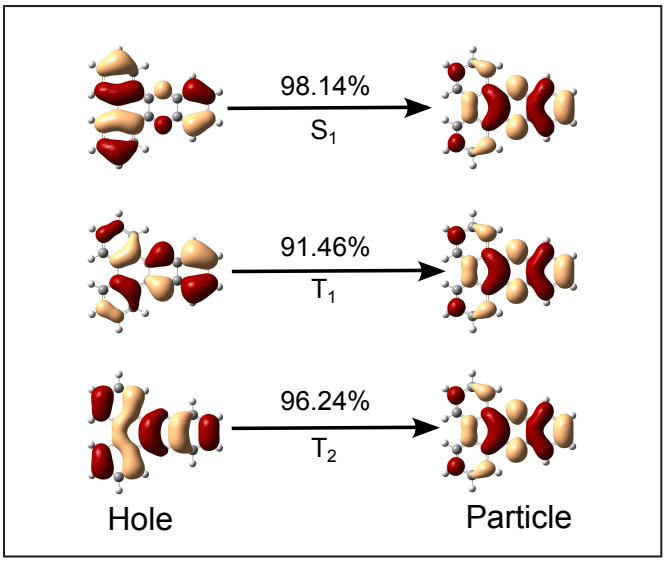

Fig. S8: NTO orbitals obtained from optimized T_2 geometry

The nature of T_2 state is of $\pi \rightarrow \pi^*$ type.

3.3 Duschisnky Rotation matrix and Displacement Vectors

This section contains the plot of Duschisky rotation matrix and Frequency vs. Displacement vector for different states.
For calculating Duschinsky rotation matrix and displacement vectors Fcclasses3[8] is used. All the calculations for DPPZ molecule regarding J and D are performed using internal co-ordinate.

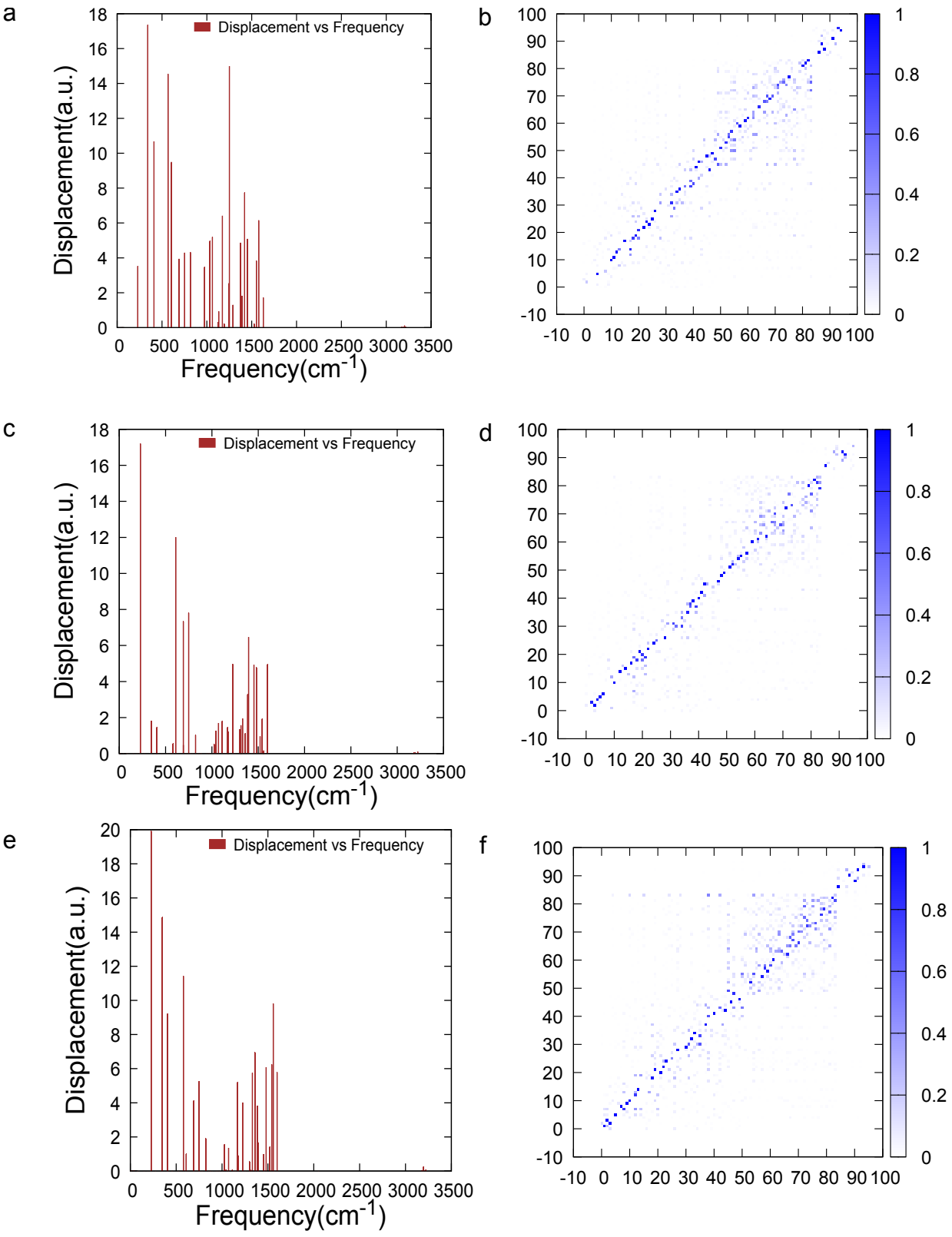
a
Displacement vs Frequency
Displacement(a.u.)
Frequency(cm-1)
b
c
Displacement vs Frequency
Displacement(a.u.)
Frequency(cm-1)
d
e
Displacement vs Frequency
Displacement(a.u.)
Frequency(cm-1)
f

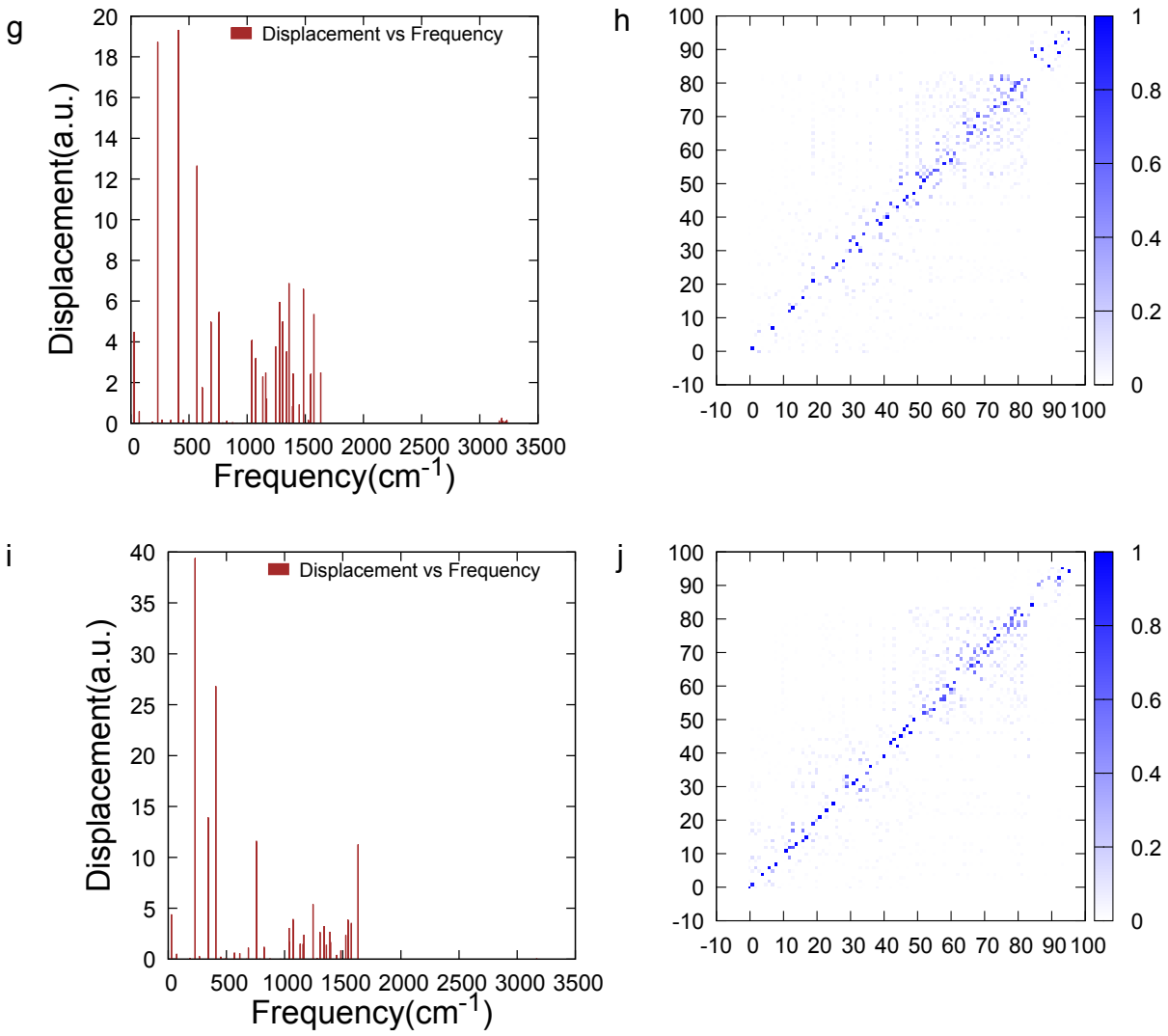

Fig. S9: a) Plot of the displacement vector for the $T_1 \rightarrow S_0$ transition versus the vibrational frequencies of the T_1 state; (b) Plot of the Duschinsky rotation matrix obtained in internal coordinates between the T_1 and S_0 states. (c) Plot of the displacement vector for the $T_2 \rightarrow S_0$ transition versus the vibrational frequencies of the T_2 state; (d) Plot of the Duschinsky rotation matrix obtained in internal coordinates between the T_2 and S_0 states. (e) Plot of the displacement vector for the $T_2 \rightsquigarrow T_1$ transition versus the vibrational frequencies of the T_2 state; (f) Plot of the Duschinsky rotation matrix obtained in internal coordinates between the T_2 and T_1 states. (g) Plot of displacement vector for the $S_1 \rightsquigarrow T_1$ transition versus the vibrational frequencies of the S_1 state; (h) Plot of the Duschinsky rotation matrix obtained in internal coordinates between the S_1 and T_1 states. (i) Plot of displacement vector for the $S_1 \rightsquigarrow T_2$ transition versus the vibrational frequencies of the S_1 state; (j) Plot of the Duschinsky rotation matrix obtained in internal coordinates between the S_1 and T_2 states.

3.4 NACME vs Frequency Plot

This section represents the variation of non-adiabatic coupling matrix elements between T_2-T_1 with respect to normal mode frequency values of T_2 state . Here it is observed that the mode specific NACME value corresponding to mode number 84 of T_2 state, having a frequency value of 2048 cm^{-1}, has highest value among other modes. This mode is contributing majorly for T_2-T_1 IC.

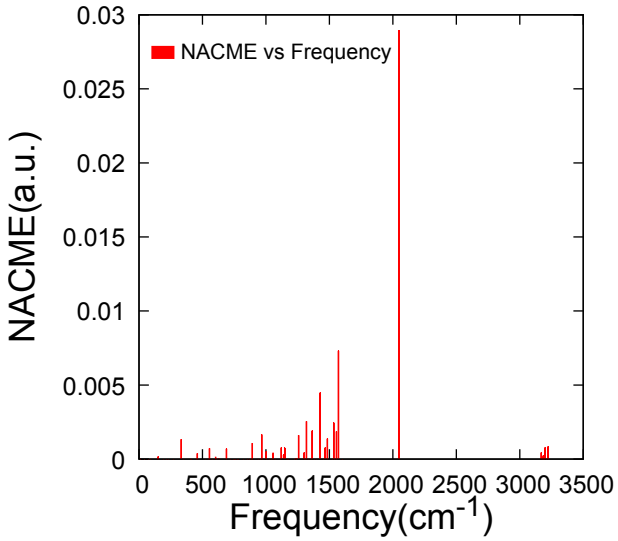

Fig. S10: Plot for NACME vs Frequency of T_2 state

3.5 Effect of Damping parameter and Temperature on the nature of phosphorescence spectra

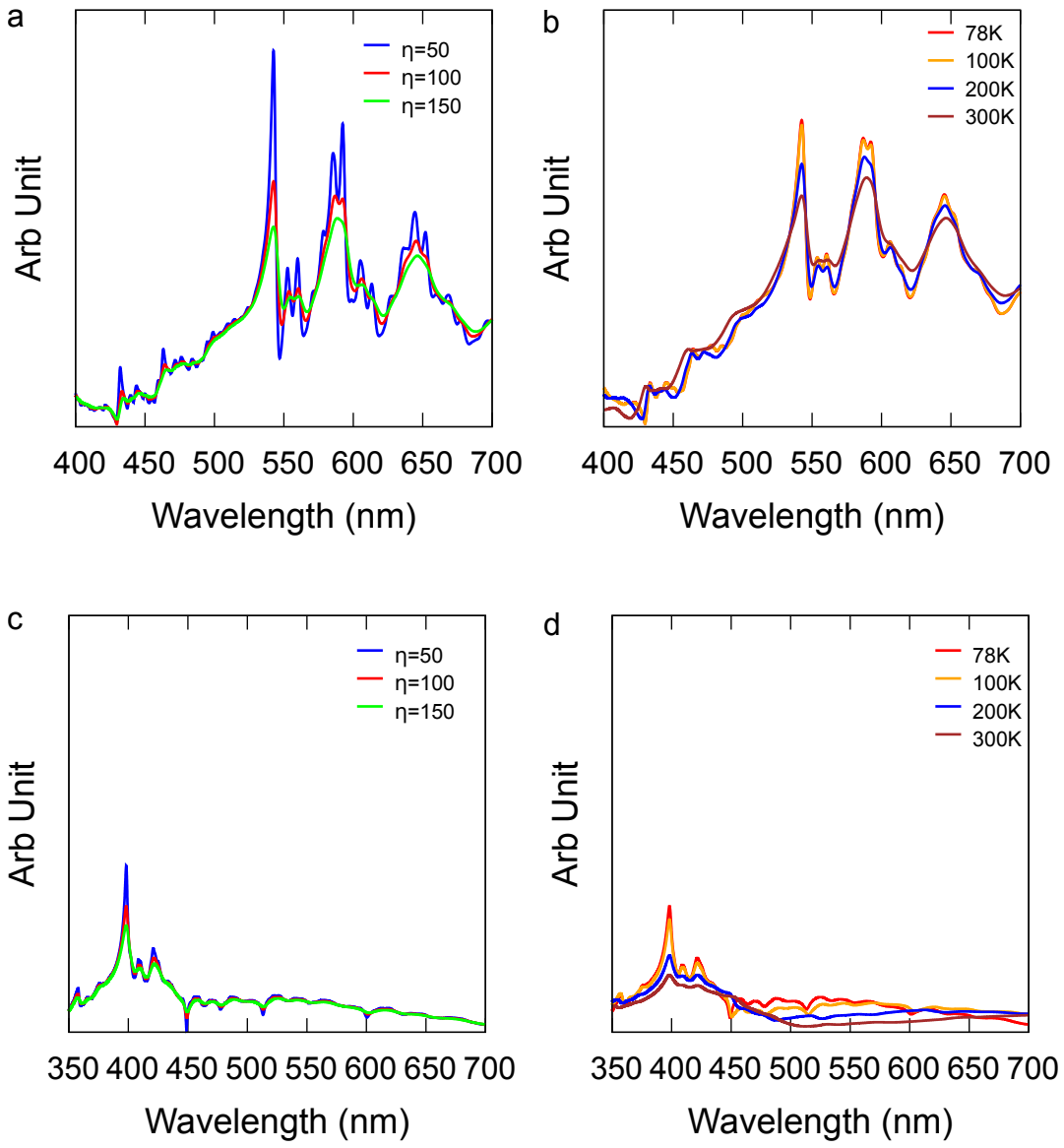

Fig. S11: Variation in the spectral features of the $T_1 \rightarrow S_0$ and $T_2 \rightarrow S_0$ phosphorescence with changes in the damping parameter (η) and temperature for the DPPZ molecule in THF solvent. (a) $T_1 \rightarrow S_0$ spectral variation, with changes in the damping parameter (in cm^{-1}). (b) $T_1 \rightarrow S_0$ spectral variation, with changes in temperature. (c) $T_2 \rightarrow S_0$ spectral variation, with changes in the damping parameter (in cm^{-1}). (d) $T_2 \rightarrow S_0$ spectral variation, with changes in temperature.

Spectral variation with respect to damping parameter and temperature difference is shown here for DPPZ molecule. Fig. S11a represents the variation of $T_1 \rightarrow S_0$ spectra of DPPZ molecule at 78 K temperature with variation of damping parameter. With increase in damping parameter the

intensity of the spectra decreases and the peaks get flattened. figure S11b shows the changes of spectral nature with changing temperature. With lowering of temperature the spectral intensity increases and the peaks get sharper.
The variation of spectral nature for $T_2 \rightarrow S_0$ phosphorescence of DPPZ molecule with respect to damping parameter and temperature is shown in Fig. S11c, Fig. S11d respectively. Both increasing η and temperature decreases the spectral intensity. The spectral simulation of $T_1 \rightarrow S_0$ and $T_2 \rightarrow S_0$ phosphorescence is done using 10^5 points and a time scale of -10ps to 10ps.

3.6 Absorption and Emission wavelengths of DPPZ molecule using def2-TZVP basis set in (6e,5o) NEVPT2 calculation

The absorption and emission wavelengths of DPPZ molecule obtained after performing a (6e,5o) NEVPT2 calculation using def2-TZVP basis set are given in tableS3. The computation of derivative SOCME using def2-TZVP basis set is computationally quite expensive. So, we have computed the SOCME, NACME and derivative SOCME for non-radiative rate constants using cc-pVDZ basis set. That is given in the manuscript.

Table S3: Absorption and emission wavelengths of DPPZ molecule obtained after performing NEVPT2 calculation taking 6 electrons and 5 orbitals and def2-TZVP basis set.

Process	**Wavelength(nm)**	**Transition moment(a.u.)**	**Expt. Result(nm)**
Absorption	366	3.82	$300 - 400$
Fluorescence	395	1.74	428
Phosphorescence ($T_1 \rightarrow S_0$)	567	0.00004	546
Phosphorescence ($T_2 \rightarrow S_0$)	419	0.00001	$400 - 500$

The experimental results are obtained from Ref. 10.

3.7 Explanation of spectral simulation in Condon only region

The expression of phosphorescence transition moment in the sum over states approach involves the product of various electronic transition moments terms between singlet-singlet/triplet-triplet and the spin orbit coupling matrix element between singlet-triplet or triplet-singlet. On the other hand, nonradiative rate constants depend on the SOCME between singlet-triplet as one of the key factors. If the electronic transition moments between the same spin states are much higher than SOCMEs, then the HT part may not be important in radiative process although it could play a vital role in the ISC process. The equation of phopshorescence transition moment in sum over states approach can be written as,

$$\boldsymbol{\mu}^{\mathrm{SOC}}_{T_1\to S_0} = \sum_n \frac{\langle S_0|\hat{\mu}|S_n\rangle\langle S_n|\hat{H}_{\mathrm{SO}}|T_1\rangle}{E(T_1)-E(S_n)} + \sum_n \frac{\langle T_1|\hat{\mu}|T_n\rangle\langle T_n|\hat{H}_{\mathrm{SO}}|S_0\rangle}{E(S_0)-E(T_n)} \tag{19}$$

$$\boldsymbol{\mu}^{\mathrm{SOC}}_{T_2\to S_0} = \sum_n \frac{\langle S_0|\hat{\mu}|S_n\rangle\langle S_n|\hat{H}_{\mathrm{SO}}|T_2\rangle}{E(T_2)-E(S_n)} + \sum_n \frac{\langle T_2|\hat{\mu}|T_n\rangle\langle T_n|\hat{H}_{\mathrm{SO}}|S_0\rangle}{E(S_0)-E(T_n)} \tag{20}$$

Table S4: Decomposition of the SOC-corrected transition dipole moment for the $T_1 \to S_0$ transition.

Intermediate State	$\langle S_0\|\hat{\boldsymbol{\mu}}\|S_n\rangle$ (a.u.)	$\langle S_n\|\hat{H}_{\mathrm{SOC}}\|T_1\rangle$ (cm^{-1})	$\langle S_n\|\hat{H}_{\mathrm{SOC}}\|T_1\rangle$ (a.u.)
S_1	1.48	0.00	0.00
S_2	3.96	0.02	9.11×10^{-8}
S_3	1.82	0.00	0.00
S_4	9.81	0.07	3.19×10^{-7}

Table S5: Decomposition of the SOC-corrected transition dipole moment for the $T_2 \to S_0$ transition.

Intermediate State	$\langle S_0\|\hat{\boldsymbol{\mu}}\|S_n\rangle$ (a.u.)	$\langle S_n\|\hat{H}_{\mathrm{SOC}}\|T_2\rangle$ (cm^{-1})	$\langle S_n\|\hat{H}_{\mathrm{SOC}}\|T_2\rangle$ (a.u.)
S_1	4.13	0.04	1.82×10^{-7}
S_2	0.99	0.00	0.00
S_3	0.32	0.01	4.56×10^{-8}
S_4	9.83	0.00	0.00

From the two tables above, the spin–orbit coupling matrix elements between singlet-triplet states are significantly smaller than the corresponding singlet–singlet transition moments. Consequently, the contribution from Herzberg–Teller coupling is likely to be weak, and the Condon approximation should provide an adequate description of the simulated spectra.

3.8 Optimized geometry coordinate and Frequencies

The coordinates of the optimized geometries of the S_0, S_1, T_1, and T_2 states are given below.

3.8.1 S_0 Geometry(Å)

N	-1.41954100	1.40388800	0.00000200
N	-1.41954100	-1.40388700	-0.00002100
C	0.98737000	2.85322600	-0.00004200
C	2.17439700	3.56164300	-0.00002200
C	3.39066200	2.86856700	0.00003500
C	3.40420300	1.48407600	0.00005300
C	3.40420300	-1.48407600	0.00000600
C	3.39066100	-2.86856700	0.00000100
C	2.17439600	-3.56164400	-0.00000500
C	0.98737000	-2.85322600	-0.00000900
C	-3.81983500	-1.41105900	-0.00002100
C	-4.99939900	-0.71034600	-0.00000300
C	-4.99939900	0.71034600	0.00002500
C	-3.81983500	1.41106000	0.00003000
C	2.20981800	0.73620900	0.00001600
C	2.20981800	-0.73620900	0.00000800
C	0.98506400	-1.44675200	-0.00000500
C	-0.28550900	-0.71896200	-0.00002100
C	-2.58121000	-0.71567800	-0.00001000
C	-2.58121000	0.71567800	0.00000800
C	-0.28550900	0.71896200	-0.00001700
C	0.98506500	1.44675200	-0.00001700
H	0.03428500	3.36486200	-0.00007700
H	2.16270400	4.64532100	-0.00004900
H	4.32768200	3.41348900	0.00006500
H	4.36076000	0.98000700	0.00010400
H	4.36075900	-0.98000700	0.00000300
H	4.32768100	-3.41349000	-0.00000100
H	2.16270300	-4.64532100	-0.00000800
H	0.03428600	-3.36486200	-0.00001800
H	-3.79725600	-2.49433200	-0.00004100
H	-5.94474500	-1.24024300	-0.00001100
H	-5.94474400	1.24024400	0.00004300
H	-3.79725500	2.49433200	0.00004900

3.8.2 Frequencies

The normal mode frequencies obtained from the optimized structure of S_0 state are given below :

31.4323	59.7879	88.9850
91.3046	150.0969	170.6848
226.9004	231.1408	298.1821
327.2580	330.0261	345.9866
408.4877	427.3078	451.2653
451.7701	456.6798	494.7976
558.1283	567.9544	572.6204
573.7497	585.8210	628.1654
629.9329	631.9157	698.0474
709.0672	715.9292	744.8026
768.0019	774.4487	774.8031
785.7545	797.1569	828.4392
833.0835	884.3569	891.1520
894.5093	908.0013	971.1015
982.8566	984.1606	989.9963
1010.9505	1011.1589	1011.8087
1018.5317	1026.0787	1057.6154
1068.2818	1085.9844	1125.4533
1145.3183	1152.3337	1168.9696
1183.5767	1184.7510	1245.0678
1248.9524	1261.3939	1269.3793
1288.0904	1323.5933	1336.8176
1346.0130	1367.4930	1374.5026
1374.7570	1425.3678	1469.1953
1477.8220	1493.9231	1500.0188
1524.6055	1531.6375	1572.4233
1580.0103	1601.7839	1617.7996
1640.5038	1647.9917	1654.9134
3170.9702	3171.9791	3173.1149
3181.8776	3184.3030	3186.5731
3191.2745	3197.2233	3197.9890
3209.0057	3209.2611	3215.6113

3.8.3 S_1 Geometry(Å)

The optimized coordinate of S_1 state is as follows:

N	-1.43277400	1.42996500	-0.00340800
N	-1.43277400	-1.42996500	0.00340800
C	0.98821400	2.81800800	-0.00235800
C	2.18389200	3.52329000	0.00016600
C	3.42505100	2.84600000	0.00509900
C	3.44602100	1.47630900	0.00571400
C	3.44602100	-1.47630900	-0.00571400

C	3.42505100	-2.84600000	-0.00509800
C	2.18389200	-3.52329000	-0.00016600
C	0.98821400	-2.81800800	0.00235800
C	-3.83437200	-1.39746800	0.00427400
C	-5.04128800	-0.69879000	0.00219600
C	-5.04128800	0.69879000	-0.00219600
C	-3.83437200	1.39746800	-0.00427400
C	2.23442200	0.71074100	0.00114700
C	2.23442200	-0.71074100	-0.00114700
C	0.97230300	-1.41932000	0.00098100
C	-0.29625400	-0.70406300	0.00139800
C	-2.59966700	-0.71927700	0.00201100
C	-2.59966700	0.71927700	-0.00201200
C	-0.29625400	0.70406300	-0.00139800
C	0.97230300	1.41932000	-0.00098100
H	0.03852400	3.33404800	-0.00500700
H	2.16596800	4.60686700	-0.00089400
H	4.35013500	3.40804500	0.00868400
H	4.39986800	0.96941900	0.01122100
H	4.39986800	-0.96941900	-0.01122100
H	4.35013500	-3.40804500	-0.00868400
H	2.16596800	-4.60686700	0.00089400
H	0.03852400	-3.33404800	0.00500700
H	-3.81598800	-2.48164900	0.00759500
H	-5.97902600	-1.24272500	0.00395400
H	-5.97902500	1.24272500	-0.00395400
H	-3.81598800	2.48164900	-0.00759500

3.8.4 Frequencies

27.3034	58.8417	72.6496
76.7013	146.8045	164.4536
186.0172	230.7334	267.5577
299.8760	327.4090	343.3803
387.4944	408.9337	420.0839
451.2499	451.3759	477.1308
493.4129	532.3688	556.3191
561.3592	568.7643	605.9470
614.3632	626.5765	673.4546
678.4343	689.2361	719.6588
723.2055	751.6102	757.7886
758.6648	780.4950	788.3527
824.0691	856.9935	874.3798
887.3775	890.1239	926.1872

961.6846	966.6912	967.6536
983.8420	1003.9162	1015.6498
1015.8404	1039.1827	1040.0110
1040.9175	1072.9325	1119.7219
1134.4657	1141.5125	1159.2855
1167.4075	1169.4144	1208.3296
1244.8473	1249.7543	1280.4470
1290.2425	1304.8640	1337.9098
1339.5439	1343.4673	1359.7606
1384.2838	1390.8496	1394.7426
1431.8687	1448.1067	1465.0586
1484.0682	1491.6074	1521.9660
1525.9369	1546.6260	1574.1111
1604.7686	1606.4196	1632.4115
3160.9979	3167.5604	3176.3040
3185.0696	3185.6576	3187.8137
3197.2944	3200.9345	3211.4739
3220.8600	3220.8981	3232.9392

3.8.5 T_1 Geometry(Å)

The coordinate of optimized T_1 state optimized through TDDFT method is as follows:

N	1.43050900	-1.42736500	-0.00000400
N	1.43050900	1.42736500	0.00000000
C	-0.98701800	-2.84647400	0.00000600
C	-2.16727100	-3.55383100	0.00001200
C	-3.39731700	-2.86694100	0.00001600
C	-3.42353400	-1.48768800	0.00001400
C	-3.42353400	1.48768800	-0.00000300
C	-3.39731700	2.86694100	-0.00000600
C	-2.16727100	3.55383100	-0.00000500
C	-0.98701800	2.84647400	-0.00000200
C	3.81537300	1.39827100	-0.00000300
C	5.05935100	0.68453200	-0.00000600
C	5.05935100	-0.68453200	-0.00001000
C	3.81537300	-1.39827200	-0.00000900
C	-2.23210200	-0.72604700	0.00000600
C	-2.23210200	0.72604700	0.00000100
C	-0.98752200	1.42971100	0.00000000
C	0.25458500	0.69972700	-0.00000100
C	2.58086300	0.71982700	-0.00000300
C	2.58086300	-0.71982700	-0.00000500
C	0.25458500	-0.69972700	-0.00000100

C	-0.98752200	-1.42971100	0.00000300
H	-0.03193300	-3.35305200	0.00000400
H	-2.15262000	-4.63770800	0.00001400
H	-4.32781400	-3.42283600	0.00002200
H	-4.38314000	-0.98881800	0.00001900
H	-4.38314000	0.98881800	-0.00000600
H	-4.32781400	3.42283600	-0.00001000
H	-2.15262000	4.63770800	-0.00000600
H	-0.03193300	3.35305200	-0.00000200
H	3.80156000	2.48155000	0.00000000
H	5.98792500	1.24170500	-0.00000600
H	5.98792500	-1.24170500	-0.00001300
H	3.80156000	-2.48155000	-0.00001200

3.8.6 Frequencies

41.7939	56.4249	90.1669
96.2921	142.9814	163.9854
207.0957	229.9030	279.6314
279.6596	309.7494	341.0603
389.8523	411.1169	415.9369
443.4594	446.7088	447.2453
501.9505	540.4192	558.7356
559.4130	567.6176	604.4914
615.2258	628.5898	659.9536
689.7840	690.5987	717.7940
738.9310	740.9766	752.4884
776.3930	781.3927	785.0154
816.6772	831.0233	866.7542
871.3001	880.3346	881.6257
918.5242	959.8389	961.9352
973.8200	976.9814	999.9718
1007.8335	1008.4568	1020.3427
1032.4187	1056.1244	1062.2098
1078.1735	1125.8364	1132.2727
1144.6617	1173.7219	1183.5379
1194.7456	1220.7392	1245.2041
1250.6438	1291.2069	1293.2455
1311.7352	1344.8966	1374.8625
1375.2827	1392.4858	1421.2926
1426.4765	1450.3540	1452.9993
1464.3461	1478.0392	1508.0030
1528.3549	1552.4007	1578.3482
1580.3460	1629.6226	1631.9161

3169.8080	3170.7700	3181.9447
3182.1711	3185.0631	3188.2192
3194.0093	3195.4946	3204.2272
3211.8023	3214.7455	3215.2026

3.8.7 T_2 Geometry(Å)

The optimized coordinate of T_2 state optimized by TDDFT method taking optimized geometry of S_0 state is given below:

N	1.41568300	-1.44024400	-0.00003900
N	1.41568300	1.44024300	-0.00001900
C	-0.97478800	-2.85635700	-0.00000900
C	-2.15444000	-3.57313800	0.00002100
C	-3.37491900	-2.88855900	0.00004800
C	-3.40199200	-1.48893300	0.00004100
C	-3.40199100	1.48893400	-0.00000600
C	-3.37491800	2.88856000	-0.00000200
C	-2.15443800	3.57313800	0.00000400
C	-0.97478700	2.85635700	-0.00000100
C	3.80957900	1.40653400	0.00001400
C	5.00223000	0.70759000	0.00002200
C	5.00223000	-0.70759100	0.00001000
C	3.80957900	-1.40653500	-0.00000900
C	-2.22878600	-0.73355300	0.00000600
C	-2.22878500	0.73355400	-0.00000200
C	-0.98062800	1.43124800	-0.00000800
C	0.26443500	0.72452400	-0.00003000
C	2.56948900	0.72803400	0.00000300
C	2.56948900	-0.72803500	-0.00000800
C	0.26443400	-0.72452400	-0.00003800
C	-0.98062900	-1.43124800	-0.00001500
H	-0.01372800	-3.35082800	-0.00003500
H	-2.13614100	-4.65630300	0.00002500
H	-4.30911700	-3.43728500	0.00007500
H	-4.36670400	-0.99962600	0.00006800
H	-4.36670400	0.99962700	-0.00001500
H	-4.30911500	3.43728600	-0.00000400
H	-2.13613900	4.65630400	0.00000900
H	-0.01372600	3.35082700	-0.00000800
H	3.79030700	2.49000500	0.00001900
H	5.94450500	1.24309100	0.00003500
H	5.94450500	-1.24309200	0.00001500
H	3.79030700	-2.49000500	-0.00002100

3.8.8 Frequencies

9.9125	39.6624	76.8870
86.3016	150.6528	152.9997
194.7344	214.6254	228.2714
272.8993	333.1437	346.5382
351.6725	403.6255	405.0027
414.7468	453.8957	459.5063
520.1466	524.2103	549.1043
555.1037	578.8886	603.5536
609.3989	627.7581	685.6444
688.8821	691.4621	691.5382
723.5127	743.7788	748.5645
762.2810	774.5266	786.4260
823.6295	854.4422	872.4514
882.0300	892.9045	939.0519
957.3235	966.8891	969.7713
971.2711	1002.2913	1002.4485
1003.0464	1024.9318	1043.3829
1056.1490	1071.2299	1110.0818
1120.6003	1138.9409	1149.4157
1167.8840	1176.0369	1224.8227
1236.0019	1257.5378	1299.0282
1300.8348	1313.5811	1319.4748
1330.6162	1359.3754	1364.0866
1385.3345	1395.6907	1426.4924
1453.5771	1464.9390	1481.5123
1483.8713	1520.0646	1534.6637
1542.1259	1555.6053	1558.3133
1571.7642	1599.9787	2048.4805
3168.8962	3176.0900	3178.0063
3179.7298	3184.8322	3188.2233
3193.2098	3194.1235	3198.8147
3211.9079	3221.8779	3221.9056

4 Flowchart describing steps involved in the theoretical calculations

The flowchart below represents a step by step explanation of the calculations performed in the study. For ground state optimization and frequency calculation DFT method is used. Excited state optimization along with frequency calculation has been performed using TDDFT level of theory. For calculating SOCME and transition dipole moment (TDM), TDDFT is used for ClB-DBT molecule and NEVPT2 for DPPZ molecule respectively. NACME calculation is performed for both the system in casscf level. After obtaining all the required input data from the performed calculations, we have used our inhouse developed code to simulate vibronic phosphorescence spectra and calculating nonradiative rate constants. In the flowchart **J**, **D** and ΔE represents the Duschinsky rotation matrix, displacement vector and energy gap between corresponding states respectively.

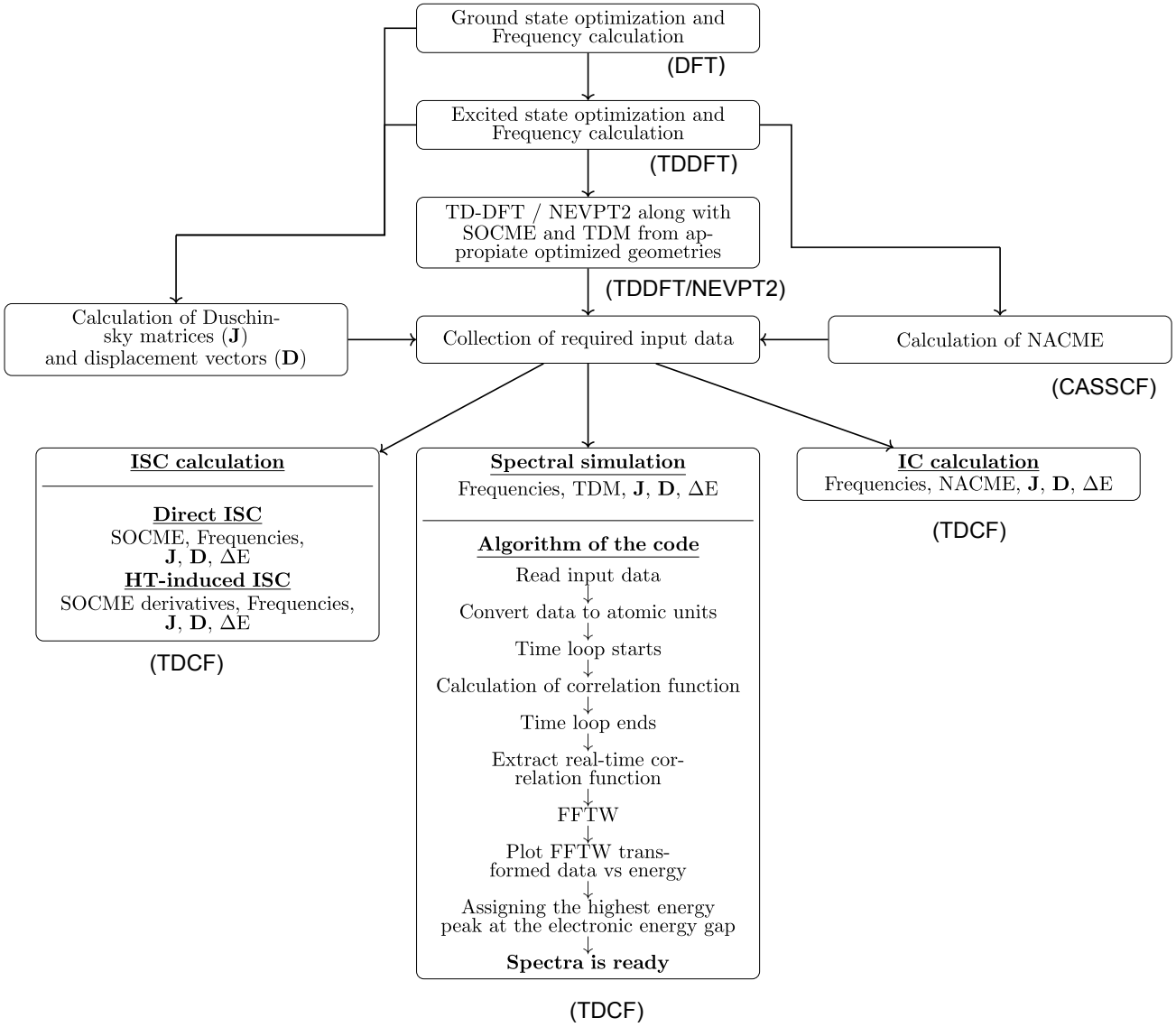

References

[1] Peng, Q.; Niu, Y.; Shi, Q.; Gao, X.; Shuai, Z. *J. Chem. Theor. Comput.* **2013**, *9*, 1132–1143.

[2] Kim, I.; Jeon, S. O.; Jeong, D.; Choi, H.; Son, W.-J.; Kim, D.; Rhee, Y. M.; Lee, H. S. *J. Chem. Theor. Comput.* **2020**, *16*, 621–632.

[3] Karak, P.; Ruud, K.; Chakrabarti, S. *J. Chem. Phys.* **2022**, *157*, 174101.

[4] Karak, P.; Moitra, T.; Chakrabarti, S. Relativistic Effects on Photodynamical Processes, 1st ed.; Elsevier: Oxford, 2024; pp 258–279.

[5] Banerjee, S.; Baiardi, A.; Bloino, J.; Barone, V. *J. Chem. Theor. Comput.* **2016**, *12*, 774–786.

[6] Peng, Q.; Yi, Y.; Shuai, Z.; Shao, J. *J. Chem. Phys.* **2007**, *126*, 114302.

[7] Karak, P.; Moitra, T.; Ruud, K.; Chakrabarti, S. *Phys. Chem. Chem. Phys.* **2023**, *25*, 8209–8219.

[8] Cerezo, J.; Santoro, F. *J. Comput. Chem.* **2023**, *44*, 626–643.

[9] Paul, L.; Moitra, T.; Ruud, K.; Chakrabarti, S. *J. Phys. Chem. Lett.* **2019**, *10*, 369–374.

[10] Zhou, C.; Zhang, S.; Gao, Y.; Liu, H.; Shan, T.; Liang, X.; Yang, B.; Ma, Y. *Adv. Funct. Mater.* **2018**, *28*, 1802407.